1-Azathioxanthone Appended Europium(III) Complexes with Excitation at 405 nm: Consequences for Lanthanide Luminescence based Bioimaging on Commercial Microscopes

Lea Gundorff Nielsen,[a,b] Anne Katrine Ravnsborg Hansen, [a] Patrycja Stachelek,[b] Robert Pal*[b] & Thomas Just Sørensen* [a]

[a] Department of Chemistry & Nano-Science Center, University of Copenhagen, Universitetsparken 5, DK2100 København Ø, Denmark, tjs@chem.ku.dk

[b] Department of Chemistry, Durham University, South Road, Durham, United Kingdom, DH1 3LE, robert.pal@dur.ac.uk

ABSTRACT: Since the pioneering report by Selvin, we have been fascinated by the potential of using lanthanide luminescence in bioimaging. The uniquely narrow emission lines and long luminescence lifetimes both provide the potential for background free images together with full certainty of probe localization. General use of lanthanide based bioimaging was first challenged by low brightness, and later by the need of UV (<405 nm) excitation sources not present in commercial microscopes. Here, three lanthanide-based imaging probes were synthesized, characterized, and used in bioimaging on dedicated as well as commercial microscopes. It was proven without doubt that the lanthanide complexes enter the cells and luminesce internally. Even so, no lanthanide luminescence were recovered on the commercial microscopes. Thus, it was concluded that even though the commercial microscopes are capable of single photon detection, lanthanide luminescence based bioimaging still requires dedicated hardware.

INTRODUCTION

Optical bioimaging is a central tool in life science.[1] Fluorescence microscopy provides information on both structure and function, but relies on fluorescent probes, either of biological origin or introduced as small molecules.[2] In commercial microscopes, the quality of the images is directly proportional to the brightness of the probe. Thus, high brightness organic and biological fluorescent probes dominate optical bioimaging.[3, 4] Two paths exist for increasing the image quality: improving dyes or improving the detection efficiency of the microscope. In the research laboratories laser excitation sources and optical detectors, where each pixel has single photon sensitivity, are common. Indeed, most commercial microscopes have these capabilities. Thus, probe development should provide the biggest potential for improvement. While the organic fluorescent probes that are commonly used have been optimised by first Drexhage,[5] Haugland,[6] and more recently Lavis,[7] other emitters—disregarding fluorescent proteins—are still to find widespread use in optical bioimaging.[4]

Since the early work by Selvin, Beeby, and Faulkner,[8, 9] the narrow emission band, long luminescence lifetime, and emission in the near-IR have made lanthanide luminescence interesting for bioimaging applications.[8, 10] Indeed, named classes of lanthanide based probes have been reported.[11] Even so, challenges remain for the exploitation of lanthanide based luminescent probes.[12] The lanthanide centred optical transitions are all forbidden, which is the origin of the long luminescence lifetimes, but also dictate very low molar absorption coefficients ($\varepsilon \leq 1$ cm^{-1} M^{-1}) *i.e.* a low brightness. This can be circumvented by sensitisation by organic chromophores,[13] where the excited state of the antenna chromophore is higher in energy than the emitting state of the lanthanide(III) ion. Using primarily europium(III) luminescence and dedicated microscopes,[14, 15, 16, 17] the benefits of the narrow emission lines and the long luminescence lifetime have been amply demonstrated.[18-20, 21] Often 355 nm (3rd Harminic of Nd:YAG) excitation is used, which requires mi-

croscopes with quartz optics and is highly phototoxic. Two-photon excitation was developed to avoid the issues with high UV-exposure,[18, 22] and while similar demonstrations of the benefits of using lanthanide based probes was reported, this method also require customized microscopes.

Following the availability of wavelength resolved detectors in commercial microscopes, we used a research microscope to show how spectral imaging can give rise to background free images.[23] We moved on to show that bioimaging following direct excitation of $\varepsilon \leq 0.1$ cm^{-1} M^{-1} bands was feasible on this dedicated platform.[24] As commercial microscopes now come equipped with highly sensitive detectors and powerful lasers light sources, we set out to demonstrate that now is the time for lanthanide based probes to shine throughout the life sciences.

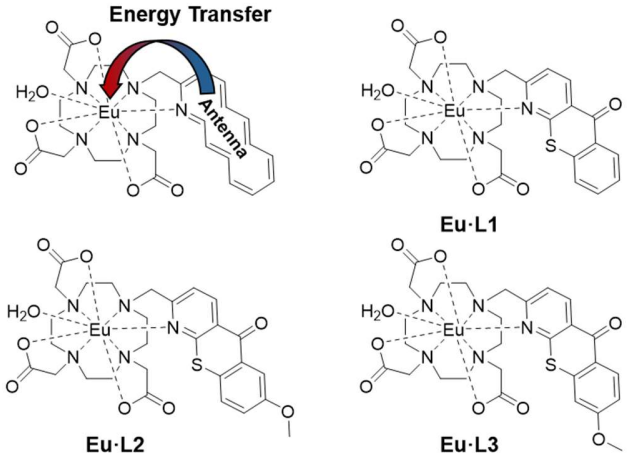

Figure 1. Illustration of the energy transfer to the Eu(III) center from the antenna and the chemical structure of the investigated Eu(III) complexes with the ligands **L1, L2** and **L3**.

When creating a lanthanide based luminescent probe, two pre-requisites have to be met: 1) the probe must sensitized following excitation of an antenna chromophore using the blue 405 nm laser line. And 2) the probe must be stable in biological media. The latter is readily ensured by using kinetically inert lanthanide binding pockets,[25] while selecting a suitable chromophore is aided by the significant contribution of Parker and co-workers.[19] Thus, we chose to make the europium(III) complexes of the 1-azathioxanthone appended 1,4,7,10-tetraazacyclododecane 1,4,7-triacetic acid ligands shown in Figure 1.

The choice of the thioxanthone chromophore class was aided by the fact that we can use Dewar's rules to predict the chromophore structure that will give us the desired photophysical properties.[26] As the photophysical properties are known to change, when the chromophore is incorporated in a lanthanide(III) ligand, we synthesized three Eu(III)-complexes. Their photophysical properties were investigated in aqueous buffered media at neutral pH mimicking biological conditions. Binding to biological proteins were tested and live cell and fixed cell imaging was the done on commercial and dedicated microscopes.

We found that the brightness of the lanthanide based probes at the point of excitation are low compared fluorescence probes, but better than any other lanthanide probe for 405 nm excitation. The probes were shown to stain cells, both live, dead and permeabilized, and beautiful cell images were recorded on microscopes dedicated to detecting lanthanide emission. However, when the same protocols were used at a facility for conventional optical bioimaging, no lanthanide emission was recovered. Following several control and model studies, it was concluded that commercial microscopes currently are biased against using lanthanide luminescence based probes. Therefore, changes in instrumentation must be in place, before we can start benefitting from the unique properties of lanthanide luminescence.

RESULTS AND DISCUSSION

Synthesis and characterization. The three 1-azathioxantone derivatives were synthesized following literature procedure through a two-step reaction.[27] Bromination in the α-position on 2-methyl-1-azathioxanone has previously been described in the literature using a Wohl—Ziegler bromination.[28, 29] However, it was not possible to reproduce this reaction in our labs. Though multiple modifications were attempted in the reaction conditions, the reaction either did not yield the desired molecules in high enough yields to continue the synthetic procedures or gave undesired products. As an alternative, a patent describing functionalization of the α-position was used with minor modifications, see SI for experimental details.[29, 30] In the preferred procedure, see Scheme 1, the parent 2-methyl-1-azathioxanthone derivatives were oxidized using iodide, iron(III)sulfate, TFA, and *tert*-butyl iodide in DMSO. The reaction was performed at least three times for each derivative, and it was shown that *tert*-butyl iodide is not required for the oxidation to occur. The reaction yields a mixture of the desired alcohol (7-9) as the minor product and the aldehyde (7a-9a) as the major product. The reaction mixture, containing both alcohol and aldehyde, was taken directly to the next step, where lithium borohydride with trimethylsilyl chloride in THF was used to reduce the sulfone and the aldehyde of the major product (7a-9a). Following the reduction, the alcohol (7-

9) was isolated after aqueous workup in an overall yield between 40-50 %. To introduce a better leaving group, the alcohol was treated with methanesulfonyl chloride, and the reactive chromophores (10-12) were isolated in acceptable yields by chromatography. The chromophore was attached to the kinetically inert DO3A-scaffold using K_2CO_3 in acetonitrile. After removal of the *tert*-butyl esters using trifluoroacetic acid, the ligands **L1**, **L2** and **L3** were isolated by tituration.[31] Finally, the Eu(III) complexes **Eu·L1**, **Eu·L2**, and **Eu·L3** were formed by complexation in a 1:1 mixture of H_2O and MeCN at neutral pH using europium(III)chloride as the Eu(III) source. The complexes were isolated following de-salting on a sephadex PD-10 column. The complexation is assumed to be quantitative, but no yields are reported as the highly hygroscopic compounds does not allow for accurate determination of absolute purity or recovered mass.[32] The formation of the Eu(III) complexes were confirmed with ^{1}H-NMR, mass spectrometry, and luminescence spectroscopy (see SI for details).

Scheme 1. Synthetic pathway to Eu(III) complex Eu·L1, Eu·L2, and Eu·L3

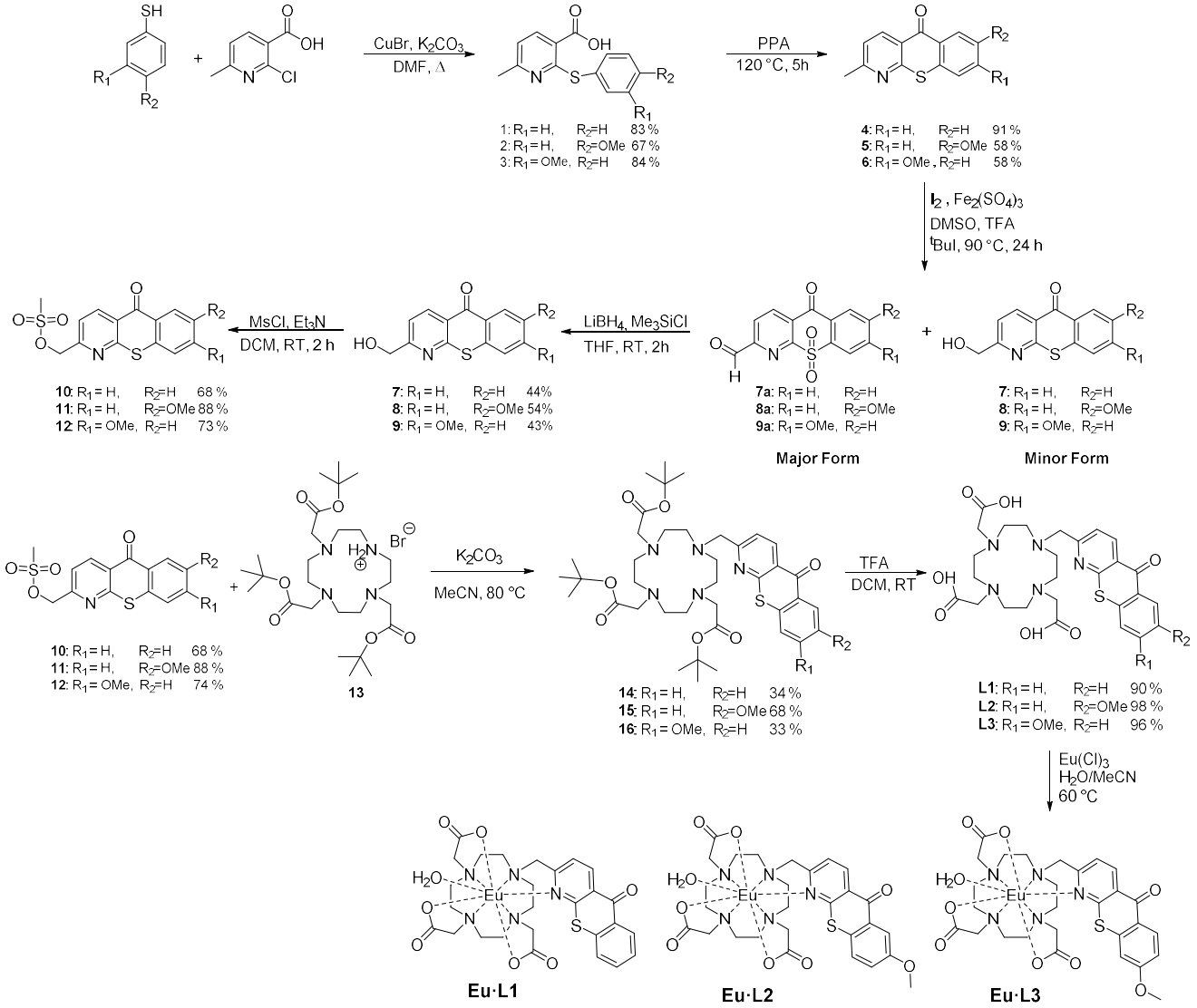

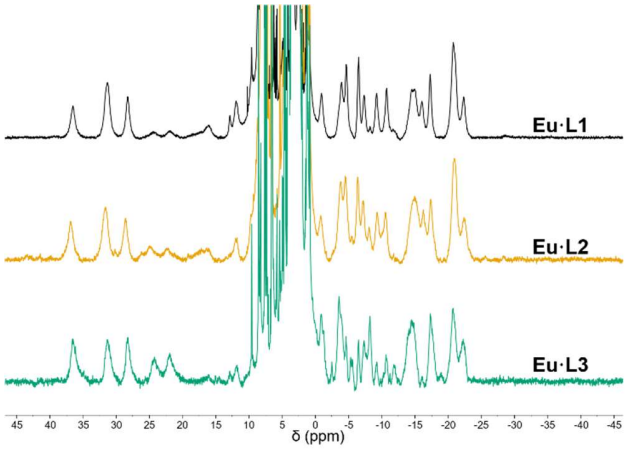

Figure 2. Paramagnetic ^{1}H-NMR of **Eu·L1** (top), **Eu·L2** (middle) and **Eu·L3** (bottom) in DMSO-d_6 at 27 °C.

Figure 2 shows the paramagnetic ^{1}H-NMR spectra of the **Eu·L1**, **Eu·L2**, and **Eu·L3** complexes recorded in DMSO- d_6. Paramagnetic ^{1}H-NMR spectra of lanthanide complexes with DOTA and DO3A-like ligands are well understood and has been characterized in detail previously.[33, 34] The spectra in Figure 2 show similar characteristics and are consistent with reported spectra of eight-coordinated unsymmetrical Eu(III) complexes with three coordinating carboxylate arms on a cyclen backbone.[35] Due to the constrained conformation of an eight-coordinated complex, fast exchange between different forms of are restricted resulting in resolution of the axial protons in the cyclen ring (25 -35 ppm).[31, 33] The NMR spectra clearly show that the Eu(III) binding pocket is similar in all three complexes.

Antenna chromophore photophysics. The photophysical properties of **Eu·L1**, **Eu·L2**, and **Eu·L3** were investigated in PBS buffer (pH 7.4) at 1.5·10^{-5} M and contrasted to the properties of the parent 1-azathioxanthone.[27] Figure 3 shows the absorption spectra, which display strong absorption in the UV range with 2-3 bands in the range of 300—400 nm. **1**, with no substituents on the azathioxanthone chromophore, has 2 bands in the range from 300—400 nm, and the primary absorption band of **1** has a maximum of 382 nm. This 12 nm redshift compared to the 1-azathioxanthone, we assign primarily to solvatochromism.[27]

Figure 3 shows that the primary absorption band of **3** has a maximum of 369 nm. The data reveals that the addition of the electron donating methoxide group in the *para*-position to the carbonyl group i.e. going from **1** to **3**, induces a blueshift of the primary ππ* transition and creates a close lying nπ* state at 315 nm. This was also seen in the parent chromophore.[27, 36]

In **Eu·L2** the methoxy substituent is in the *para*-position to the bridging sulfur atom. This induces a redshift of the absorption maximum and creates a chromophore with a maximum absorption at 403 nm, close to the 405 nm central wavelength of the blue laser line commonly used in commercial microscopes.

Figure 3 shows that the excitation spectra of all three complexes exclusively show the primary band of the chromophore. No bands arising from direct excitation of the Eu(III) center can be seen. Further, the excitation spectra are identical to the absorption spectra. Note that the absorption spectrum of **1** extends into the blue and can be excited using a 405 nm laser. All photophysical details of the antenna chromophores are compiled in Table 1, and the corresponding data can be found in the SI. Note that the mirror image rule works for **1** and **3**, while a second band on the red is seen for **2**. This is assigned to ligand centered phosphorescence.[27, 36]

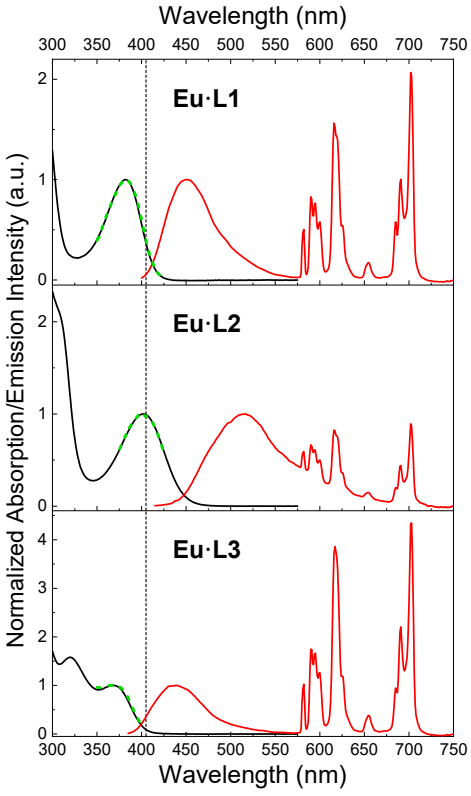

Figure 3. Normalized absorption (black), excitation (dashed green on top of absorption) and emission (red) spectra of **Eu ·L1** (λ_{ex} 380, λ_{em} 701), **Eu·L2** (λ_{ex} 405, λ_{em} 701) and **Eu·L3** (λ_{ex} 370, λ_{em} 701) in PBS buffer pH 7.4 at 1.5·10^{-5} M. The black vertical dashed line is positioned at 405 nm, to show the central excitation wavelength in a blue laser.

Table 1. Photophysical properties of **Eu ·L1**, **Eu·L2** and **Eu·L3** determined in PBS solution at pH 7.4. See SI for details.

	1	**2**	**3**
λ_{abs} (nm)	382	403	369
λ_{fl} (nm)	452	517	440
E_S (cm^{-1})	24240	22560	25030
E_T (cm^{-1})	22500	19800	23040
ΔS_1-T_1 (cm^{-1})	1360	2519	1990
$<\tau_{fl}>$ (ns)	3.67	8.3	0.61
Φ_{fl} (%)	9.3	6.9	2.1
Φ_{lum}(%)	2.8	0.8	2.5
Log(ε) at λ_{max}	3.8	3.7	3.8
B at λ_{max}	188	44	174
Log(ε) at λ_{405}	3.0	3.7	2.0
B at λ_{405}	26	42	2.5
τ (H_2O) (ms)	0.604	0.256	0.539
τ (D_2O) (ms)	1.753	0.424	2.017
q	1.0 ±0.5	-	1.3 ±0.5

Eu(III) photophysics. The emission spectra shown in Figure 3 have the characteristic europium centered luminescence on the red side of ligand fluorescence and phosphorescence. The narrow emission lines of the europium luminescence report on the local symmetry.[37] The fine structure is very similar in all three spectra, which confirms the observation from NMR, that the three complexes have similar coordination geometry and solution structure.[33, 35]

A prerequisite for efficient lanthanide sensitization is energy overlap between donor and acceptor states. Thus, the relative energies of the excited states involved in the energy transfer cascade leading to the lanthanide-centered luminescence must be considered for the three complexes. Figure 4 shows the energy levels of the first excited singlet (E_S) and triplet (E_T) states of **Eu·L1**, **Eu·L2** and **Eu·L3** compared to the lowest excited energy levels for the europium(III) aqua ion. In the three complexes sensitization from S_1 and T_1 are viable mechanisms considering the overlap of energy levels.[38] Back energy transfer from europium(III) to the antenna chromophore is unlikely as the energy gap is higher than 2000 cm^{-1}.[39]

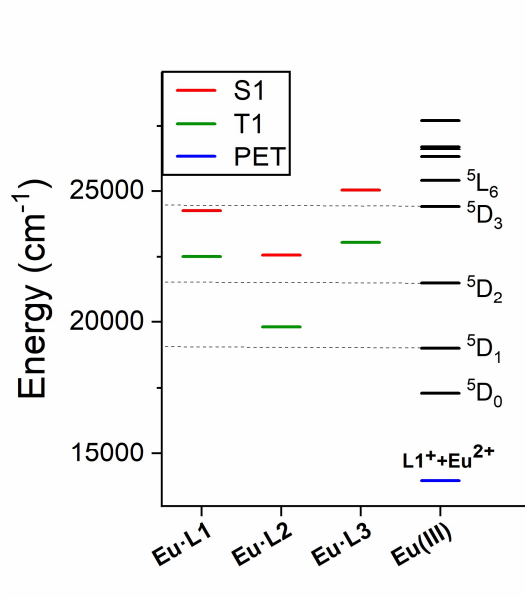

Figure 4. Energy diagram for **Eu·L1**, **Eu·L2**, and **Eu·L3** together with the energy levels of Eu(III).[40] Solid lines show excited singlet (red), triplet (green), approximate redox level (blue), and energy levels of Eu(III) (black). The dashed black line is used to compare the energy between the excited states on the antenna to that of Eu(III). The reduction potentials used in the figure are EuIII/EuII = −0.35 V in water vs. NHE and for thioxanthone in DMF: 1.62 V vs. NHE.[29, 41]

The luminescence lifetimes were measured in PBS (pH = 7.4) prepared from H_2O and D_2O to determine the number of solvent molecules coordinated to the europium(III) center using the modified Horrocks' equation.[42] The lifetimes of **1** and **3** are as expected, while the lifetime of too short. This is assigned to back energy transfer to the triplet state T_1 2500 cm^{-1} over the $^5D_0$ state, most likely mediated by thermal population of the $^5D_1$ level.

For **1** and **3** q, the number of coordinating solvent molecules, can be calculated and the average number of coordinating water molecules is 1 for both complexes. This indicates that the chromophore pendant arm is coordinating the lanthanide center.[43]

1 and 2 as luminescent probes. The key photophysical properties of the complexes are compiled in table 1. The quantum yield for the organic fluorescence (Φ_{fl}) and the Eu(III)-centered emission excited through the antenna (Φ_{lum}) were determined by the dilution method.[44] The Eu(III) luminescence quantum yields were found to be in the range of 0.5-3 %. For luminescent probes it is important to contrast the quantum yield to the molar absorption coefficient in order to evaluate the efficiency of the complex as a probe. This can be evaluated as the brightness ($B = \varepsilon(\lambda_{ex}) \cdot QY$). While

the brightness of **1** and **2** are low compared to organic fluorophores (~100 vs ~100.000), it is greatly improved when compared to a Eu(III) complex with no antenna appended. Compared to EuDOTA an increase of a factor 10.000-100.000 is observed.[45] Note that **Eu·L2** has the lowest brightness of the complexes at the primary absorption maximum, but the highest brightness at 405 nm. Due to the redshift in absorption, **Eu·L2** becomes the brightest luminescent probe.

In biological samples, binding of proteins will change the property of luminescent probes.[46] This was investigated by incremental addition of bovine serum albumin (BSA) to **Eu·L1**, **Eu·L2**, and **Eu·L3** while maintaining constant concentration of the complex, see supporting information. The results are summarized in Table 2. For **Eu·L1** and **Eu·L3** the Eu(III) luminescence is reduced by half, while it for **Eu·L2** is increased 3.5-fold.

Table 2. Relative change in ligand fluorescence and Eu(III) luminescence after addition of 20 mg/mL BSA.

	I(with BSA)/I(in buffer)	
	Em_{Ligand}	Em_{Eu}
Eu·L1	0.26	0.43
Eu·L2	0.89	3.56
Eu·L3	1.29	0.56

Cell imaging. **Eu·L1** and **Eu·L2** were investigated for use in bioimaging. **Eu·L3** was not used as the absorption maximum is in the UV-region. The complexes were investigated with high resolution Laser Scanning Confocal Microscopy (LSCM) images recorded on a modified Leica SP5 II microscope, equipped with a SIM technique called PhMoNa at Durham University.[15] Cell uptake and co-localization studies were done for **Eu·L1** and **Eu·L2** in living mouse skin fibroblasts (NIH-3T3). Both **Eu·L1** and **Eu·L2** permeated into the NIH-3T3 cells when loaded in DMEM (Dulbecco's modified Eagle's medium) with 10 % FBS (fetal bovine serum) and 1% pen strep at 37 ° in 5% CO_2/air. Incubation times from 2-24 hours were tested together with concentrations ranging from 12.5 μM up to 50 μM. The cells remained visible healthy over the full period of examination of up to 24 h with 50 μM loading concentration.

Colocalization experiments were done using Mitotracker Green and Lysotracker Green to confirm the localization of the Eu(III) complexes in the cell. Mitotracker Green confirmed that the complexes were predominantly localized in the mitochondria (Figure 5).

The cells stained with the two Eu(III) complexes were all excited using a 405 nm laser and the images were measured with detection from 570 -700 nm where only Eu(III) luminescence is emitted cf. Figure 3. To further confirm that the emission observed from the cells originated from the Eu(III) center, and not from the antenna or background fluorescence, time-resolved emission spectra were measured from the cells stained with **Eu·L1**: The cell slides were placed on a custom built specialized inverted microscope adapted to allow for time-gated imaging and spectroscopy.[16] Due to instrumental limitations, these spectra were recorded using 355 nm excitation. Figure 5 shows the steady state spectrum and the time-gated spectrum, which both clearly display the Eu(III) luminescence following excitation of the ligand. These spectra confirm that **Eu·L1** permeates the cells and that the images recorded on the dedicated microscope arise from Eu(III) luminescence.

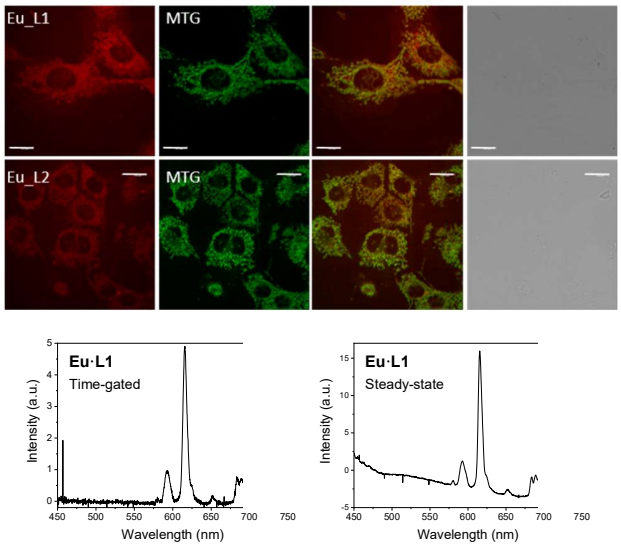

Figure 5. Top panel: 50 uM **Eu·L1** incubated for 4 h. Middle panel: 50 uM **Eu·L2** incubated for 24 h. Co-staining with mitotracker green (P = 0.74 and 0.69 respectively). Transmission images are shown for each row confirming cell viability. All cell images are obtained with 405 nm excitation. Scale bars represent to 20 μm. Bottom left: Time-gated emission spectrum of **Eu·L1** excited at 355 nm with 20 μs gate time.[16] Bottom right: Steady-state emission spectrum of **Eu·L1** excited at 355 nm.

To test the luminescent probes on a conventional microscope, we used the Core Facility for Integrated Microscopy at the University of Copenhagen. Here, cell uptake studies were done on formaldehyde fixed HeLa cells permeabilized with Triton X stained with 50 μM dye. The images were obtained using a Zeiss Confocal microscope LSM 780 where an emission profile of the luminescence detected was obtained together with the cell

image using a 405 nm laser, f-MBS:405/505c or f-MBS:405/565c beam splitter, and the 32-channel detector without any additional optical elements. For **Eu·L2** no signal was obtained from the stained cells. For **Eu·L1** bright images of cell nuclei were recorded, see figure 6A. The images obtained were compared with DAPI stained cells to confirm to localization of the complex in the nuclei, see SI. The emission profile obtained directly from the cell images on the microscope did not reveal any Eu(III) luminescence (Figure 6C). However, when the same cover slide with the stained cells were placed in the fluorimeter, the characteristic Eu(III) luminescence with emission bands at 595 nm and 620 nm were observed (Figure 6D). This clearly demonstrates uptake of the Eu(III)-complex in the cell, and that the issue is the microscope, not the luminescent probe. These experiments were replicated with live cells with the same result.

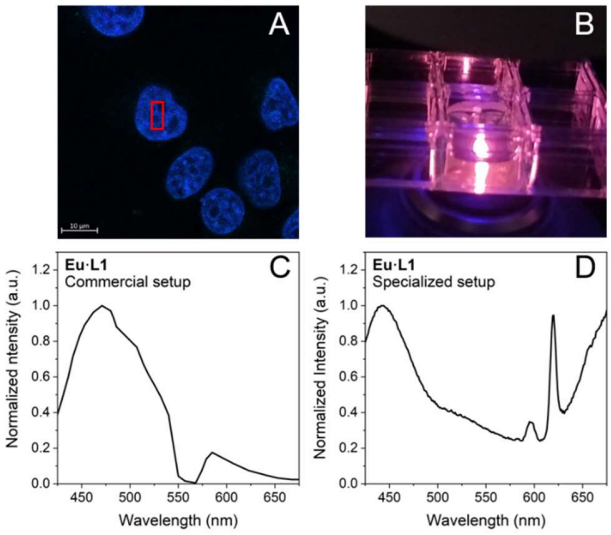

Figure 6. A: 50 μM **Eu·L1** stained cell. B: Image of emitted light from a 150 μM **Eu·L1** solution in PBS. C: Emission profile of the luminescence collected from the nuclei (red square, 7A). The spectrum was obtained from LSM 780 microscope. D: Steady state emission spectrum of the same cell slide obtained from a fluorimeter. All images and spectra are obtained with 405 nm excitation. A, B, and C are using identical settings on the same microscope.

The experiments done on the LSM 780 microscope indicated that the commercial setup was not able to detect the Eu(III) luminescence in cells. To test the capability of the instrument to detect the sharp emission lines originating from Eu(III), an emission profile was obtained directly of a solution of the dye. Figure 6B shows that the pink color of Eu(III) luminescence was easily observed with the eye. We went on to show that at high concentration, peaks around 590 nm and 620 nm can be detected on the microscope, see supporting information.

ICP-MS analysis was used to confirm that the uptake of Eu(III) in the cell for both **Eu·L1** and **Eu·L2** documenting that the complexes are present in the cells. Perfect ignore comment above) To further support this conclusion—and in addition to the spectra in Figure 5—the luminescence lifetime of the **Eu·L1** complex was determined in the cells. The luminescence lifetime decreases to 99 μs in cells. This is significantly less than the 604 μs luminescence lifetime in PBS, and lower than the 239 μs determined in pure DMEM cell media. This indicates strong quenching effects from both cell media and the cell biology, which is not unexpected since Eu(III) luminescence is strongly affected by the chemical environment.[21, 47]

Conclusion

Three lanthanide based luminescent probes were synthesized, characterized and their performance in bioimaging was investigated in great detail. While high quality images of the mitochondria was recorded using Eu(III) luminescence on a dedicated microscope, no Eu(III) luminescence was recorded on conventional commercial microscopes. It was clearly shown that europium(III) was present in the investigated cell samples, and did luminesce in the cells. Thus we conclude that at the current state of development, conventional fluorescence microscopes are not suitable platforms for lanthanide based bioimaging.

ASSOCIATED CONTENT

Synthetic procedurec and characterization of all new compounds, additional photophysical characterization, and detailed discussion of ligand syntheses and complexation procedures (PDF)

AUTHOR INFORMATION

Corresponding Author

* tjs@chem.ku.dk
* robert.pal@dur.ac.uk

Funding Sources

TJS and LGN acknowledges support from Carlsberg-foundation, Villum Fonden (Grant#14922), Novo Nordisk Fonden, Eliteforsk, and the University of Copenhagen.
RP acknowledges support from the Royal Society University Research Fellowship URF\R\191002 H2020-MSCA-ITN-859752 HEL4CHIROLED and BBSRC BB/S017615/1 and BB/X001172/1.

ACKNOWLEDGMENT

We acknowledge the Core Facility for Integrated Microscopy, Faculty of Health and Medical Sciences, University of Copenhagen.
We thank the Carlsbergfoundation, Villum Fonden, Novo Nordisk Fonden, Eliteforsk, and the University of Copenhagen for generous support.
We thank Stefan Warthegau for assistance in the preparation of the manuscript.

REFERENCES

(1) Montero Llopis, P.; Senft, R. A.; Ross-Elliott, T. J.; Stephansky, R.; Keeley, D. P.; Koshar, P.; Marqués, G.; Gao, Y.-S.; Carlson, B. R.; Pengo, T.; et al. Best practices and tools for reporting reproducible fluorescence microscopy methods. *Nature Methods* **2021**, *18* (12), 1463-1476. DOI: 10.1038/s41592-021-01156-w.

(2) Farkas, D. L. Invention and commercialization in optical bioimaging. *Nat Biotech* **2003**, *21* (11), 1269-1271, 10.1038/nbt1103-1269. Stephens, D. J.; Allan, V. J. Light microscopy techniques for live cell Imaging. *Science* **2003**, *300* (5616), 82-86, Review. Hell, S. W. Far-field optical nanoscopy. *Science* **2007**, *316* (5828), 1153-1158, Review. Johnsson, N.; Johnsson, K. Chemical tools for biomolecular imaging. *ACS Chem. Bio.* **2007**, *2* (1), 31-38, Review. DOI: 10.1021/cb6003977.

(3) Lavis, L. D.; Raines, R. T. Bright ideas for chemical biology. *ACS Chem. Biol.* **2008**, *3* (3), 142-155, Review. DOI: 10.1021/cb700248m. Grimm, J. B.; Lavis, L. D. Caveat fluorophore: an insiders' guide to small-molecule fluorescent labels. *Nature Methods* **2022**, *19* (2), 149-158. DOI: 10.1038/s41592-021-01338-6. Specht, E. A.; Braselmann, E.; Palmer, A. E. A Critical and Comparative Review of Fluorescent Tools for Live-Cell Imaging. *Annual Review of Physiology* **2017**, *79*, 93-117, Review. DOI: 10.1146/annurev-physiol-022516-034055 Scopus. Giepmans, B. N. G.; Adams, S. R.; Ellisman, M. H.; Tsien, R. Y. Review - The fluorescent toolbox for assessing protein location and function. *Science* **2006**, *312* (5771), 217-224, Review. DOI: 10.1126/science.1124618.

(4) Haugland, R. P. *Handbook of Fluorescent Probes and Research Chemicals*; Molecular Probes, 2010.

(5) Drexhage, K. H. STRUCTURE AND PROPERTIES OF LASER-DYES. *Top. Appl. Phys.* **1973**, *1*, 144-193, Review.

(6) Sun, W.-C.; Gee, K. R.; Klaubert, D. H.; Haugland, R. P. Synthesis of Fluorinated Fluoresceins. *The Journal of Organic Chemistry* **1997**, *62* (19), 6469-6475. DOI: 10.1021/jo9706178. Panchuk-Voloshina, N.; Haugland, R. P.; Bishop-Stewart, J.; Bhalgat, M. K.; Millard, P. J.; Mao, F.; Leung, W. Y. Alexa dyes, a series of new fluorescent dyes that yield exceptionally bright, photostable conjugates. *J. Histochem. Cytochem.* **1999**, *47* (9), 1179-1188, Article.

(7) Grimm, J. B.; Muthusamy, A. K.; Liang, Y.; Brown, T. A.; Lemon, W. C.; Patel, R.; Lu, R.; Macklin, J. J.; Keller, P. J.; Ji, N.; et al. A general method to fine-tune fluorophores for live-cell and in vivo imaging. *Nat Methods* **2017**, *14* (10), 987-994. DOI: 10.1038/nmeth.4403.

(8) Vereb, G.; Jares-Erijman, E.; Selvin, P. R.; Jovin, T. M. Temporally and Spectrally Resolved Imaging Microscopy of Lanthanide Chelates. *Biophys J* **1998**, *74* (5), 2210-2222.

(9) Faulkner, S.; Beeby, A.; Dickins, R. S.; Parker, D.; Williams, J. A. G. Generating a warm glow: Lanthanide complexes which luminesce in the near-IR. *Journal of fluorescence* **1999**, *9* (1), 45-49. DOI: Doi 10.1023/A:1020535707477. Beeby, A.; Botchway, S. W.; Clarkson, I. M.; Faulkner, S.; Parker, A. W.; Parker, D.; Williams, J. A. G. Luminescence imaging microscopy and lifetime mapping using kinetically stable lanthanide(III) complexes. *Journal of Photochemistry and Photobiology B-Biology* **2000**, *57* (2-3), 83-89. DOI: Doi 10.1016/S1011-1344(00)00070-1.

(10) Selvin, P. R. Principles and biophysical applications of lanthanide-based probes. *Annu Rev Biophys Biomol Struct* **2002**, *31*, 275-302. DOI: 10.1146/annurev.biophys.31.101101.140927. Heffern, M. C.; Matosziuk, L. M.; Meade, T. J. Lanthanide probes for bioresponsive imaging. *Chem Rev* **2014**, *114* (8), 4496-4539. DOI: 10.1021/cr400477t. Bunzli, J. C. Lanthanide luminescence for biomedical analyses and imaging. *Chem Rev* **2010**, *110* (5), 2729-2755. DOI: 10.1021/cr900362e. Montgomery, C. P.; Murray, B. S.; New, E. J.; Pal, R.; Parker, D. Cell-penetrating metal complex optical probes: targeted and responsive systems based on lanthanide luminescence. *Acc Chem Res* **2009**, *42* (7), 925-937. DOI: 10.1021/ar800174z. Moore, E. G.; Samuel, A. P.; Raymond, K. N. From antenna to assay: lessons learned in lanthanide luminescence. *Acc Chem Res* **2009**, *42* (4), 542-552. DOI: 10.1021/ar800211j. Sun, L. D.; Wang, Y. F.; Yan, C. H. Paradigms and challenges for bioapplication of rare earth upconversion luminescent nanoparticles: small size and tunable emission/excitation spectra. *Acc Chem Res* **2014**, *47* (4), 1001-1009. DOI: 10.1021/ar400218t.

(11) Butler, S. J.; Lamarque, L.; Pal, R.; Parker, D. EuroTracker dyes: highly emissive europium complexes as alternative organelle stains for live cell imaging. *Chemical Science* **2014**, *5* (5), 1750-1756, 10.1039/C3SC53056F. DOI: 10.1039/C3SC53056F.

(12) Sørensen, T. J.; Faulkner, S. Metal Ions in Bio-Imaging Techniques. In *5 Lanthanide Complexes Used for Optical Imaging*, Astrid, S., Eva, F., Roland, K. O. S. Eds.; De Gruyter, 2021; pp 137-156.

(13) Weissman, S. I. Intramolecular Energy Transfer The Fluorescence of Complexes of Europium. *The Journal of chemical physics* **1942**, *10* (4), 214-217. DOI: 10.1063/1.1723709. Kleinerman, M. Energy Migration in Lanthanide Chelates. *The Journal of chemical physics* **1969**, *51* (6), 2370-2381. DOI: 10.1063/1.1672355.

(14) Nonat, A.; Bahamyirou, S.; Lecointre, A.; Przybilla, F.; Mely, Y.; Platas-Iglesias, C.; Camerel, F.; Jeannin, O.; Charbonniere, L. J. Molecular Upconversion in Water in Heteropolynuclear Supramolecular Tb/Yb Assemblies. *Journal of the American Chemical Society* **2019**, *141* (4), 1568-1576. DOI: 10.1021/jacs.8b10932. Liao, Z.; Tropiano, M.; Faulkner, S.; Vosch, T.; Sørensen, T. J. Time-resolved confocal microscopy using lanthanide centred near-IR emission. *RSC Adv.* **2015**, (5), 70282–70286. DOI: 10.1039/c5ra15759e. Liao, Z.; Tropiano, M.; Mantulnikovs, K.; Faulkner, S.; Vosch, T.; Just Sørensen, T. Spectrally resolved confocal microscopy using lanthanide centred near-IR emission. *Chemical Communications* **2015**, *51* (12), 2372-2375. DOI: 10.1039/C4CC09618E.

(15) Pal, R. Phase modulation nanoscopy: a simple approach to enhanced optical resolution. *Faraday Discussions* **2015**, *177* (0), 507-515, 10.1039/C4FD00158C. DOI: 10.1039/C4FD00158C.

(16) Pal, R.; Beeby, A. Simple and versatile modifications allowing time gated spectral acquisition, imaging and lifetime profiling on conventional wide-field microscopes. *Methods and applications in fluorescence* **2014**, *2* (3), 037001. DOI: 10.1088/2050-6120/2/3/037001.

(17) Stachelek, P.; MacKenzie, L.; Parker, D.; Pal, R., Circularly polarised luminescence laser scanning confocal microscopy to study live cell chiral molecular interactions. Nature Communications 2022, 13 (1), 553.

(18) Picot, A.; D'Aléo, A.; Baldeck, P. L.; Grichine, A.; Duperray, A.; Andraud, C.; Maury, O. Long-Lived Two-Photon Excited Luminescence of Water-Soluble Europium Complex: Applications in Biological Imaging Using Two-Photon Scanning Microscopy. *Journal of the American Chemical Society* **2008**, *130* (5), 1532-1533. DOI: 10.1021/ja076837c (acccessed 2015/02/17).

(19) Yu, J. H.; Parker, D.; Pal, R.; Poole, R. A.; Cann, M. J. A europium complex that selectively stains nucleoli of cells. *Journal of the American Chemical Society* **2006**, *128* (7), 2294-2299. DOI: Doi 10.1021/Ja056303g.

(20) Petoud, S.; Cohen, S. M.; Bunzli, J. C. G.; Raymond, K. N. Stable lanthanide luminescence agents highly emissive in aqueous solution: Multidentate 2-hydroxyisophthalamide complexes of SM3+, Eu3+, Tb3+, Dy3+. *Journal of the American Chemical Society* **2003**, *125* (44), 13324-13325. DOI: Doi 10.1021/Ja0379363. Foucault-Collet, A.; Gogick, K. A.; White, K. A.; Villette, S.; Pallier, A.; Collet, G.; Kieda, C.; Li, T.; Geib, S. J.; Rosi, N. L.; et al. Lanthanide near infrared imaging in living cells with Yb3+ nano metal organic frameworks. *Proceedings of the National Academy of Sciences of the United States of America* **2013**, *110* (43), 17199-17204. DOI: 10.1073/pnas.1305910110. Pershagen, E.; Borbas, K. E. Multiplex detection of enzymatic activity with responsive lanthanide-based luminescent probes. *Angewandte Chemie* **2015**, *54* (6), 1787-1790. DOI: 10.1002/anie.201408560. Martin, K. E.; Cosby, A. G.; Boros, E. Multiplex and In Vivo Optical Imaging of Discrete Luminescent Lanthanide Complexes Enabled by In Situ Cherenkov Radiation Mediated Energy Transfer. *Journal of the American Chemical Society* **2021**, *143* (24), 9206-9214. DOI: 10.1021/jacs.1c04264. Cardoso Dos Santos, M.; Colin, I.; Ribeiro Dos Santos, G.; Susumu, K.; Demarque, M.; Medintz, I. L.; Hildebrandt, N. Time-Gated FRET Nanoprobes for Autofluorescence-Free Long-Term In Vivo Imaging of Developing Zebrafish. *Advanced Materials* **2020**, *32* (39), 2003912. DOI: https://doi.org/10.1002/adma.202003912.

(21) Kovacs, D.; Lu, X.; Meszaros, L. S.; Ott, M.; Andres, J.; Borbas, K. E. Photophysics of Coumarin and Carbostyril-Sensitized Luminescent Lanthanide Complexes: Implications for Complex Design in Multiplex Detection. *Journal of the American Chemical Society* **2017**, *139* (16), 5756-5767. DOI: 10.1021/jacs.6b11274.

(22) Xiong, R.; Mara, D.; Liu, J.; Van Deun, R.; Borbas, K. E. Excitation- and Emission-Wavelength-Based Multiplex Spectroscopy Using Red-Absorbing Near-Infrared-Emitting Lanthanide Complexes. *Journal of the American Chemical Society* **2018**, *140* (35), 10975-10979. DOI: 10.1021/jacs.8b07609.

(23) Carro-Temboury, M. R.; Arppe, R.; Hempel, C.; Vosch, T.; Just Sørensen, T. Creating infinite contrast in fluorescence microscopy by using lanthanide centered emission. *Plos One* **2017**, *12* (12), e0189529. DOI: 10.1371/journal.pone.0189529.

(24) Arppe-Tabbara, R.; Carro-Temboury, M. R.; Hempel, C.; Vosch, T.; Sørensen, T. J. Luminescence from Lanthanide(III) Ions Bound to the Glycocalyx of Chinese Hamster Ovary Cells. *Chemistry – A European Journal* **2018**, *24* (46), 11885-11889. DOI: doi:10.1002/chem.201802799.

(25) Sørensen, T. J.; Faulkner, S. Multimetallic Lanthanide Complexes: Using Kinetic Control To Define Complex Multimetallic Arrays. *Acc Chem Res* **2018**, *51* (10), 2493-2501. DOI: 10.1021/acs.accounts.8b00205. Caravan, P.; Ellison, J. J.; McMurry, T. J.; Lauffer, R. B. Gadolinium(III) chelates as MRI contrast agents: Structure, dynamics, and applications. *Chemical Reviews* **1999**, *99* (9), 2293-2352. DOI: Doi 10.1021/Cr980440x. Wahsner, J.; Gale, E. M.; Rodríguez-Rodríguez, A.; Caravan, P. Chemistry of MRI Contrast Agents: Current Challenges and New Frontiers. *Chemical Reviews* **2019**, *119* (2), 957-1057. DOI: 10.1021/acs.chemrev.8b00363.

(26) Dewar, M. J. S. 478. Colour and constitution. Part I. Basic dyes. *Journal of the Chemical Society* **1950**, 2329-2334. Griffiths, J. *Colour and Constitution of Organic Molecules*; Academic Press, 1976. Junker, A. K. R.; Sørensen, T. J. Rationalizing substituent effects in 1-Azathioxanthone photophysics. *Methods and applications in fluorescence* **2018**, *6*, 014002. DOI: 10.1088/2050-6120/aa9c16.

(27) Junker, A. K. R.; Sørensen, T. J. Rationalizing substituent effects in 1-azathioxanthone photophysics. *Methods and Applications in Fluorescence* **2017**, *6* (1), 014002.

(28) Atkinson, P.; Findlay, K. S.; Kielar, F.; Pal, R.; Parker, D.; Poole, R. A.; Puschmann, H.; Richardson, S. L.; Stenson, P. A.; Thompson, A. L.; et al. Azaxanthones and azathioxanthones are effective sensitisers for europium and terbium luminescence. *Organic & Biomolecular Chemistry* **2006**, *4* (9), 1707-1722, 10.1039/B601357K. DOI: 10.1039/B601357K.

(29) Verma, P.; Sawant, R. M.; Pal, H. Intriguing multichannel photoinduced electron transfer in lanthanide (iii)–diphenylamine systems. *Physical Chemistry Chemical Physics* **2015**, *17* (35), 23214-23225.

(30) Parker, D.; Pal, R.; Yu, J. Responsive luminescent lanthanide complexes. 2012.

(31) Junker, A. K. R.; Deblonde, G. J.-P.; Abergel, R. J.; Sørensen, T. J. Investigating subtle 4f vs. 5f coordination differences using kinetically inert Eu (iii), Tb (iii), and Cm (iii) complexes of a coumarin-appended 1, 4, 7, 10-tetraazacyclododecane-1, 4, 7-triacetate (DO3A) ligand. *Dalton transactions* **2018**, *47* (21), 7362-7369.

(32) Sørensen, T. J.; Tropiano, M.; Blackburn, O. A.; Tilney, J. A.; Kenwright, A. M.; Faulkner, S. Preparation and study of an f,f,f',f'' covalently linked tetranuclear hetero-trimetallic complex - a europium, terbium, dysprosium triad. *Chem Commun (Camb)* **2013**, *49* (8), 783-785. DOI: 10.1039/c2cc35931f. Sørensen, T. J.; Kenwright, A. M.; Faulkner, S. Bimetallic lanthanide complexes that display a ratiometric response to oxygen concentrations. *Chemical Science* **2015**, *6* (3), 2054-2059, 10.1039/C4SC03827D. DOI: 10.1039/C4SC03827D.

(33) Nielsen, L. G.; Sørensen, T. J. Including and Declaring Structural Fluctuations in the Study of Lanthanide(III) Coordination Chemistry in Solution. *Inorganic Chemistry* **2019**. DOI: 10.1021/acs.inorgchem.9b01571.

(34) Jacques, V.; Desreux, J. F. Quantitative Two-Dimensional EXSY Spectroscopy and Dynamic Behavior of a Paramagnetic Lanthanide Macrocyclic Chelate: YbDOTA(DOTA = 1,4,7,10-Tetraazacyclododecane-N,N',N'',N'''-tetraacetic Acid). *Inorganic Chemistry* **1994**, *33* (18), 4048-4053. DOI: 10.1021/ic00096a033. Desreux, J. F. Nuclear magnetic resonance spectroscopy of lanthanide complexes with a tetraacetic tetraaza macrocycle. Unusual conformation properties. *Inorganic Chemistry* **1980**, *19* (5), 1319-1324. DOI: 10.1021/ic50207a042. Aime, S.; Botta, M.; Ermondi, G. NMR study of solution structures and dynamics of lanthanide(III) complexes of DOTA. *Inorganic Chemistry* **1992**, *31* (21), 4291-4299. DOI: 10.1021/ic00047a016. Aime, S.; Botta, M.; Fasano, M.; Marques, M. P. M.; Geraldes, C. F. G. C.; Pubanz, D.; Merbach, A. E. Conformational and Coordination Equilibria on DOTA Complexes of Lanthanide Metal Ions in Aqueous Solution Studied by 1H-NMR Spectroscopy. *Inorganic Chemistry* **1997**, *36* (10), 2059-2068. DOI: 10.1021/ic9613640.

(35) Junker, A. K.; Tropiano, M.; Faulkner, S.; Sorensen, T. J. Kinetically Inert Lanthanide Complexes as Reporter Groups for Binding of Potassium by 18-crown-6. *Inorganic Chemistry* **2016**, *55* (23), 12299-12308. DOI: 10.1021/acs.inorgchem.6b02063.

(36) Arppe, R.; Kofod, N.; Junker, A. K. R.; Nielsen, L. G.; Dallerba, E.; Just Sørensen, T. Modulation of the Photophysical Properties of 1-Azathioxanthones by Eu3+, Gd3+, Tb3+, and Yb3+ Ions in Methanol. *European Journal of Inorganic Chemistry* **2017**, *2017* (44), 5246-5253. DOI: 10.1002/ejic.201700720.

(37) Binnemans, K. Interpretation of europium(III) spectra. *Coordination Chemistry Reviews* **2015**, *295*, 1-45. DOI: 10.1016/j.ccr.2015.02.015.

(38) Yang, C.; Fu, L.-M.; Wang, Y.; Zhang, J.-P.; Wong, W.-T.; Ai, X.-C.; Qiao, Y.-F.; Zou, B.-S.; Gui, L.-L. A Highly Luminescent Europium Complex Showing Visible-Light-Sensitized Red Emission: Direct Observation of the Singlet Pathway. *Angewandte Chemie International Edition* **2004**, *43* (38), 5010-5013, https://doi.org/10.1002/anie.200454141. DOI: https://doi.org/10.1002/anie.200454141 (acccessed 2022/06/16). Eliseeva, S. V.; Bünzli, J.-C. G. Lanthanide luminescence for functional materials and bio-sciences. *Chemical Society Reviews* **2010**, *39* (1), 189-227, 10.1039/B905604C. DOI: 10.1039/B905604C.

(39) Nielsen, L. G.; Junker, A. K. R.; Sorensen, T. J. Composed in the f-block: solution structure and function of kinetically inert lanthanide(III) complexes. *Dalton Transactions* **2018**, 10.1039/C8DT01501E. DOI: 10.1039/C8DT01501E.

(40) Carnall, W.; Fields, P.; Rajnak, K. Electronic energy levels of the trivalent lanthanide aquo ions. IV. Eu3+. *The Journal of Chemical Physics* **1968**, *49* (10), 4450-4455.

(41) Aruga, T.; Ito, O.; Matsuda, M. Effect of the oxidation number of the sulfur atom on the thioxanthone radical anions studied by electronic absorption and ESR spectra. *Journal of the American Chemical Society* **1979**, *101* (25), 7585-7589.

(42) Supkowski, R. M.; Horrocks Jr, W. D. On the determination of the number of water molecules, q, coordinated to europium(III) ions in solution from luminescence decay lifetimes. *Inorganica Chimica Acta* **2002**, *340*, 44-48. DOI: https://doi.org/10.1016/S0020-1693(02)01022-8. Beeby, A.; M. Clarkson, I.; S. Dickins, R.; Faulkner, S.; Parker, D.; Royle, L.; S. de Sousa, A.; A. Gareth Williams, J.; Woods, M. Non-radiative deactivation of the excited states of europium, terbium and ytterbium complexes by proximate energy-matched OH, NH and CH oscillators: an improved luminescence method for establishing solution hydration states. *Journal of the Chemical Society, Perkin Transactions 2* **1999**, (3), 493-504, 10.1039/A808692C. DOI: 10.1039/A808692C.

(43) Junker, A. K. R.; Sørensen, T. J. Shining light on the excited state energy cascade in kinetically inert Ln(iii) complexes of a coumarin-appended DO3A ligand. *Dalton Transactions* **2019**, *48* (3), 964-970, 10.1039/C8DT04464C. DOI: 10.1039/C8DT04464C.

(44) Würth, C.; Grabolle, M.; Pauli, J.; Spieles, M.; Resch-Genger, U. Relative and absolute determination of fluorescence quantum yields of transparent samples. *Nat. Protocols* **2013**, *8* (8), 1535-1550, Protocol. DOI: 10.1038/nprot.2013.087

http://www.nature.com/nprot/journal/v8/n8/abs/nprot.2013.087.html#supplementary-information. Brouwer, A. M. Standards for photoluminescence quantum yield measurements in solution (IUPAC Technical Report). *Pure Appl. Chem.* **2011**, *83* (12), 2213-2228. DOI: 10.1351/pac-rep-10-09-31.

(45) manuscript in preperation

(46) Law, G.-L.; Man, C.; Parker, D.; Walton, J. W. Observation of the selective staining of chromosomal DNA in dividing cells using a luminescent terbium(iii) complex. *Chemical Communications* **2010**, *46* (14), 2391-2393, 10.1039/B924679G. DOI: 10.1039/B924679G. Wang, X.; Wang, X.; Wang, Y.; Guo, Z. Terbium(iii) complex as a luminescent sensor for human serum albumin in aqueous solution. *Chemical Communications* **2011**, *47* (28), 8127-8129, 10.1039/C1CC12429C. DOI: 10.1039/C1CC12429C. Mailhot, R.; Traviss-Pollard, T.; Pal, R.; Butler, S. J. Cationic Europium Complexes for Visualizing Fluctuations in Mitochondrial ATP Levels in Living Cells. *Chemistry – A European Journal* **2018**, *24* (42), 10745-10755. DOI: 10.1002/chem.201801008.

(47) Kovacs, D.; Borbas, K. E. The role of photoinduced electron transfer in the quenching of sensitized Europium emission. *Coordination Chemistry Reviews* **2018**, *364*, 1-9. DOI: https://doi.org/10.1016/j.ccr.2018.03.004. Kovacs, D.; Mathieu, E.; Kiraev, S. R.; Wells, J. A. L.; Demeyere, E.; Sipos, A.; Borbas, K. E. Coordination Environment-Controlled Photoinduced Electron Transfer Quenching in Luminescent Europium Complexes. *Journal of the American Chemical Society* **2020**, *142* (30), 13190-13200. DOI: 10.1021/jacs.0c05518.

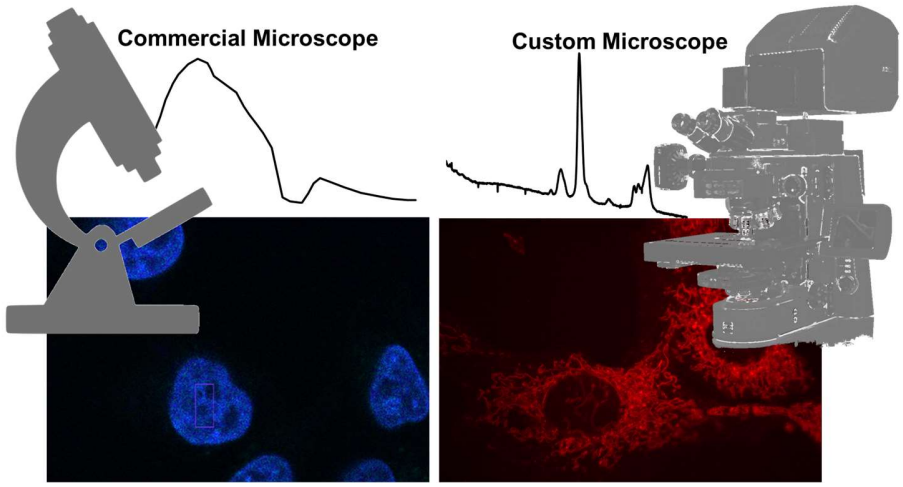
Commercial Microscope
Custom Microscope